The effect of an Acid-sensing ion channel 3 (ASIC3) inhibitor on pain-related behavior by nucleus pulposus applied on the nerve root in rats

The effect of an Acid-sensing ion channels (ASICs) inhibitor on pain-related behavior by nucleus pulposus applied on the nerve root in rats

Yoshihiro Kobayashi, Miho Sekiguchi, Shin-ichi Konno

Department of Orthopaedic Surgery, Fukushima Medical University School of Medicine, Fukushima, Japan,

Address correspondence to: Miho Sekiguchi, MD, PhD
Department of Orthopedic Surgery, Fukushima Medical University School of Medicine
1- Hikarigaoka, Fukushima City, Fukushima 960-1295, Japan
Fax: +81-24-548-5505
Tel: +81-24-547-1276
E-mail: miho-s@fmu.ac.jp

Acknowledgements: The author thanks Takuya Kameda, Akira Sato, Kei Fukanuma and Kazuo Sasaki for their technical assistance.

IRB approval/Research Ethics Committee: There is no potential conflict in this study.

Abstract

Study Design: Controlled, interventional, animal study.

Objective: To examine the effect of an inhibitor of acid-sensing ion channel 3 (ASIC3) on pain-related behavior induced by application of the nucleus pulposus (NP) onto the dorsal root ganglion (DRG) in rats.

Summary of Background Data: ASIC3 is associated with acidosis pain in inflamed or ischemic tissues and is expressed in sensory neurons and NP cells. The ASIC3 inhibitor, APETx2, increases the mechanical threshold of pain in models of knee osteoarthritis or postoperative pain. However, the efficacy of APETx2 for pain relief in the NP application model remains unknown.

Methods; Autologous NP was applied to the left L5 nerve root of 183 adult female Sprague-Dawley rats. The DRGs were treated with NP plus one of the following four treatments: saline solution (SM), low (0.01μg: LD), medium (0.1μg: MD), or high dose (1.0μg: HD) of APETx2. Behavioral testing was performed to investigate the mechanical withdrawal threshold using von Frey hairs. Expression of nerve growth factor, hypoxia-inducible factor-1α (HIF1α), activating transcription factor-3, and ionized calcium-binding adaptor molecule-1 was evaluated using immunohistochemistry. Statistical differences among multiple groups were assessed using the Steel test, the Tukey–Kramer test, and the Dunnett test. p values less than 0.05 were considered significant.

Results; The thresholds in the HD group were higher than those in the SM group at Days 14 and 21 ($p < 0.05$). In the MD group, the threshold was higher than in the SM group at Day 14 ($p < 0.05$). High doses of APETx2 reduced the expression of HIF1α after Day 14 compared to the SM group ($p < 0.05$).

Conclusion; APETx2 significantly improved pain-related behavior in a dose-dependent manner. APETx2 may inhibit ASIC3 and partly inhibit Nav1.8 channels. This ASIC3 channel inhibitor may be a potential therapeutic agent in early-stage lumbar disc herniation.

INTRODUCTION

Lumbar disc herniation (LDH) is one of the most common orthopedic diseases, afflicting many patients with lower back pain, sciatica, and paralysis of lower limbs. The prevalence of LDH is 1% of the general population, with 2,800,000 herniations per year in the United States[1]. The size of the herniated disc does not correspond to LDH symptoms, and a high prevalence (20-76%) of asymptomatic LDH has been reported [2,3]. Therefore, not only mechanical factors but also chemical factors are considered to be causes for inducing radiculopathy. The nucleus pulposus (NP) contains inflammatory mediators such as tumor necrosis factor-alpha, interleukin-1-beta, interleukin-6, serotonin, nitric oxide, and nerve growth factor (NGF) [4-14]. The model of application of autologous NP does not have a mechanical impact on the nerve, and pain is predominantly due to chemical factors[17]. In some experimental studies, application of NP[14-18] or chemical factors[4-6,19] increases endoneurial fluid pressure[20], reduces blood flow, and induces inflammation, ischemia (hypoxia inducible factor 1-alpha; HIF1α) [21], tissue acidosis [22], and changes in ion channels[23,24] in dorsal root ganglia (DRGs) and pain-related behavior in rats. Furthermore, in terms of electrophysiological neuronal activity, ion channels, particularly sodium channels, are a focus in pain research and are considered important[23,24]. Acid-sensing ion channels (ASICs), which are sodium channels that belong to the DEGenerin/Epithelial Na^+ Channel (DEG/ENaC) family, are activated by low extracellular pH and

are associated with acidosis pain in inflamed or ischemic tissues[22-35], particularly ASIC3, which is mainly expressed in sensory neurons[36,37]. ASIC3 expression in DRGs was reported in the rat NP model; lidocaine improves the reduction in the pain threshold and suppresses ASIC3 expression in the DRGs[38]. These results suggest that ASIC3 inhibition may be effective for pain relief in patients with lumbar disc herniation. The sea anemone peptide toxin, APETx2, which is an ASIC3 inhibitor[39], blocks the decrease in intra-gastric pH and histopathological changes in an acute gastric mucosal lesion model [40] and increases the mechanical threshold in a knee osteoarthritis model[41] and a postoperative pain model[42] in rats. However, no reports have been published on the effect of APETx2 against pain-related behavior induced by NP application on the nerve root in rats. The purpose of this study was to investigate the effect of APETx2 on pain-related behavior induced by the NP in rats.

MATERIALS AND METHODS

The animal experiments were carried out following the approval of the Animal Care and Use Committee in accordance with the Guidelines for Animal Experiments of our university and the Japanese Ministry of the Environment for Law Concerning the Protection and Control of Animals.

Animals and surgical procedures[15-18]

A total of 183 adult female Sprague–Dawley rats (180-220 g; Japan SLC, Shizuoka, Japan) were housed in plastic cages at room temperature (21-24°C) with a 12-hour light–dark cycle with free access to food and water. The animals were anesthetized with intraperitoneal injection of 0.1 ml/100 g of mixed anesthetic (0.3 mg medetomidine hydrochloride, 4.0 mg midazolam, and 5.0 mg butorphanol tartrate). The L5 DRG and spinal nerve were exposed by a L5/6 facetectomy. The autologous NP was harvested from the disc of the coccygeal spine and applied to the DRG (NP group). Sham animals underwent the same procedure without NP application to the DRG (sham group). Then, the spinal muscles were sutured, and the skin was closed using metal clips.

Drug administration

The ASIC3 inhibitor, APETx2 (Alomone Labs, Jerusalem, Israel), is a peptide toxin produced by the sea anemone, *Anthopleura elegantissima*. The concentration of APETx2 was adjusted using saline as a solvent. Animals in the NP group were divided into four sub-groups: the saline group (SM), the low-dose APETx2 group (0.01 μg, LD), the medium-dose APETx2 group (0.1 μg, MD), and the high-dose APETx2 group (1.0 μg, HD) (Table 1). Each animal was administered 0.05 ml drug or saline into the underlayer of the epineurium just distal to the NP at the time of surgery.

Behavioral testing

To test pain-related behavior, sensitivity to non-noxious mechanical stimulation was measured in the treatment groups (n = 12 per group) using the von Frey test. The rats were placed in a transparent plastic box with a wire netting floor and were allowed to acclimatize for 15 minutes. The mid-plantar surface of the left hind paw was stimulated using von Frey filaments (1.0-26.0 g force; monofilament sensory tester, SAKAI Med, Tokyo, Japan). Stimulation was initiated with the 1.0-g filament, and filaments were sequentially applied to the surface of the paw just until the filament bent and was held for approximately 3 seconds. The response was considered positive if the rat lifted its hind limb and showed licking or shaking of the foot as an escape response. Behavior tests were performed at Days 0 (baseline), 2, 7, 14, 21, and 28 after surgery.

Immunoblotting

Immunoblotting for ASIC3 was performed every 7 days for 28 days (n = 6 per group). Naive rats were used as controls (n = 3). The rats were rapidly decapitated under anesthesia, and the left L5 DRGs were removed and frozen in liquid nitrogen. Samples were homogenized in lysis buffer (Cell Signaling Technology, Danvers, MA, USA) containing 2.2 mg/ml 2-mercaptoethanol (SIGMA-ALDRICH, St. Louis, MO, USA). The total protein concentration for each sample was measured using a bicinchoninic acid protein assay kit (Pierce, Rockford, IL, USA). Proteins were separated on a 10% electrophoretic

gel (20 mg/lane) (Wako Pure Chemical Industries, Osaka, Japan) in Tris–glycine-SDS buffer (1.5 hours, 100 V), and then they were transferred to polyyinylidene difluoride filter membranes (EMD Millipore Corporation, Billerica, MA, USA) for 3 hours at 0.08 mA. Then, the membranes were incubated overnight in diluted primary antibody in 5% bovine serum, 1× Tris-buffered saline, and 0.1% Tween-20 at 4°C with gentle shaking. The following primary and secondary antibodies were used: rabbit anti-ASIC3 (1:2000; Alomone Labs) and goat anti-rabbit IgG conjugated to horseradish peroxidase (1:5000; Santa Cruz Biotechnology Inc., Dallas, TX, USA). Positive bands were visualized using an enhanced chemiluminescence system (ImageQuant LAS 4000, GE Healthcare UK Ltd., Buckinghamshire, England). The signal of positive bands was calculated relative to internal control signals (β-actin-positive bands) using an imaging analysis system (ImageQuant TL, GE Healthcare UK Ltd.). The ratio in naive rats was considered to be 1.

Immunohistochemistry

Immunohistochemistry for HIF1α as a marker of ischemia, activating transcription factor-3 (ATF-3) as a marker of axonal damage, NGF as a marker of a pain-related substance, and ionized calcium-binding adaptor molecule-1 (Iba-1) as a marker of activated microglia was performed on postoperative Days 7, 14, and 21 (n = 6 per group). The rats were euthanized using isoflurane (Wako Pure Chemical Industries), perfused with a fresh

solution of 4% paraformaldehyde in 0.1 M phosphate-buffered saline (PBS), and the left L5 DRG and spinal cord (SC) were removed and subsequently embedded in paraffin. Two sections (6 μm thick) were cut from each DRG and placed on separate slides. Sections were deparaffinized with xylene and rehydrated with 100% ethanol, followed by PBS. After that, they were pretreated with Dako Target Retrieval Solution (Dako North America, Carpinteria, CA, USA) at 97°C for 20 minutes to enhance immunoreactivity (IR). Samples were incubated in 2% normal goat serum in PBS/0.3% Triton X-100 for 1 hour at room temperature. Rabbit anti-ATF3 (1:100; Santa Cruz Biotechnology Inc.), anti-HIF1α antibody (1:500; Santa Cruz Biotechnology Inc.), rabbit anti-NGF antibody (1:100; NOVUS BIOLOGICALS, Littleton, CO, USA), or rabbit anti-Iba-1 antibody (1:200; Wako) was applied, and samples were incubated overnight at 4°C, followed by PBS washing. Next, samples were incubated for 1 hour at room temperature with donkey anti-goat or goat anti-rabbit Alexa Flour 488 fluorescent antibody (green) (1:200; Molecular Probes, Eugene, OR, USA). Fluorescent staining was analyzed using a BX53 fluorescent microscope (Olympus, Tokyo, Japan) equipped with a digital camera DP73 (Olympus) using the software "cellSens" (Olympus). NGF-, HIF1α-, and ATF3-positive cells and all DRG neurons were counted on each slide, and the percentage of positive cells was calculated. The number of Iba-1-positive cells in the spinal dorsal horn was counted and normalized to the constant area (0.16 mm^2) in each of five SC slides.

Statistical analysis

All data are reported as the mean ± standard deviation (SD). Statistical differences between two groups were compared using the Wilcoxon test. Statistical differences among multiple groups were assessed using the Steel test, the Tukey–Kramer test, and the Dunnett test. P values less than 0.05 were considered significant.

RESULTS

Behavioral testing (Figure 1)

The mechanical withdrawal threshold in the SM group was decreased for up to 28 days. In the HD group, the threshold significantly improved at Days 14 and 21 compared to that of the SM group ($p < 0.05$). In the MD group, the threshold was significantly increased at Day 14 ($p < 0.05$). We observed no significant differences in the threshold between the SM and LD groups.

Immunoblotting for ASIC3

No significant differences were observed in ASIC3 intensity among the treatment groups at any time point (Figure 2).

Immunohistochemical analyses

The number of NGF-IR neurons in the NP group was higher than in the sham

group at Days 7 and 14 ($p < 0.05$) (Figure 3a). The numbers of NGF-IR neurons in both the MD and HD groups were significantly lower than in the SM group ($p < 0.05$) (Figure 3b). The number of ATF-3-IR neurons in the NP group was higher compared with the sham group at Days 7 and 14 ($p < 0.05$) (Figure 4a). In the NP treatment groups, we found no significant difference in ATF-3 expression at any time point (Figure 4b). The ratio of HIF1α-IR neurons was higher in the NP (non-treatment) group compared to the sham group ($p < 0.05$) (Figure 5a). In the HD group, the ratio of HIF1α-IR neurons was significantly lower compared to that of the SM group ($p < 0.05$) (Figure 5b). The number of Iba1-IR microglia in the SC was higher in the NP group compared with that in the sham group at each time point ($p < 0.05$) (Figure 6a). We found no significant difference in Iba1-IR expression among the four treatment groups at any time point (Figure 6b).

DISCUSSION

This study showed the effect of medium and high doses of APETx2 on improving pain-related behavior induced by application of the NP to the rat nerve root. ASIC3 is formed by homo- or heteromeric association of six different subunits: ASIC1a[43], ASIC1b[44], ASIC2a[45,46], ASIC2b[47], ASIC3[25,27,36], and ASIC4[48, 49]. Various combinations of subunits have been reported: heteromeric ASIC3+1a, ASIC3+1b, and ASIC3+2b. The half-maximal 50% inhibitory concentration (IC_{50}) of APETx2 has been reported, and different

concentrations of APETx2 have inhibitory effects on each heteromeric combination of ASIC3 subunits [39]. The dose of APETx2 (0.044 μM) in the LD group was lower than the IC_{50} of the ASIC3 homomeric association (63 nM). APETx2 (0.44 μM) in the MD group has a higher affinity for homomeric ASIC3 (IC_{50}: 63 nM) and ASIC3+2b (IC_{50}: 117 nM) channels. Furthermore, APETx2 (4.4 μM) in the HD group has higher affinity for ASIC3+1a (IC_{50}: 2 μM), ASIC3+1b (IC_{50}: 0.9 μM), and ASIC3+2b. Therefore, these findings suggest that pain-related behavior improved after treatment with medium and high doses of APETx2 in a dose-dependent manner.

Spontaneous neural activity in the DRGs[50] and abnormal discharge in dorsal horn neurons are observed in electrophysiological studies after application of NP[51], and Nav1.8-IR and Nav1.9-IR neurons increase in the DRGs in a rat disc herniation model [53]. Nav1.8 is inhibited by APETx2 (IC_{50}: 2.6 μM) [52], a concentration of APETx2 close to that in the HD group. Thus, APETx2 may affect pain-related behavior through both heteromeric associations of ASIC3 subunits and/or Nav1.8. However, Nav1.8-IR neurons are increased only at day 1 [53], and therefore, one of the limitations of this study is that the functions of ASIC3 and Nav1.8 channels were not investigated with electrophysiological techniques, such as the whole-cell patch clamp system.

ASIC3 was expressed in this study, and the threshold improved 7 days after administration of APETx2. We observed a time-lag between administration of APETx2 and improvement of the threshold. Therefore, other factors may

also affect pain-related behavior. Iba-1-IR microglia in the SC increased 7 days after application of NP. However, APETx2 had no effect on microglia. Microglia play an important role in neuropathic pain, especially chronic pain. These observations suggest that the inhibitor of ASIC3 and/or the voltage-dependent sodium channels does not affect chronicity of radiculopathy.

Levels of inflammatory cytokines, interleukins, and pH change the nerve microenvironment due to LDH. In a study of cultured degenerated human intervertebral discs, interleukins, matrix metalloproteinases, Toll-like receptors, NGF, etc. are present in the NP [54,55]. Chemical factors, such as serotonin and tumor necrosis factor-alpha, play key roles and interact with each other in the early phase, and pain-related behavior induced by the NP is longer lasting than a single application of either chemical factor in the LDH model[19, 56]. NP may induce various conditions and different degrees of inflammation. ASIC3 is expressed in NP cells of the intervertebral disc and plays a key role in protecting NP cells at a low pH. Suppression of ASIC3 induces NP cell apoptosis [57, 58]. In this study, NGF and HIF1α expression was lower after APETx2 treatment. In addition, we found no difference in the expression of a nerve damage marker (ATF-3) in DRGs among the treatment groups. Thus, APETx2 inhibits ASIC3 activity in the applied NP rather than the DRGs, and a decrease in NP cell survival may lead to a decreased influence of inducing inflammation from the NP to the DRGs, leading to improvement in pain-related behavior with medium and high doses of

APRTx2. Furthermore, epigalocatechin 3-gallate (EGCG) inhibits the expression of proinflammatory mediators and matrix metalloproteinases in an *in vitro* intervertebral disc cell culture study, as well as radiculopathic pain *in vivo*[55]. The time course of pain-related behavior after EGCG treatment is similar to that in this study. EGCG, which was applied to the DRGs, may inhibit the inflammatory response of NP tissue, and may have less influence on the DRGs than the expression of cytokines and pain-related inflammation. Therefore, although pain-related behavior is induced, the thresholds recover earlier than that in the non-treatment group. This time course of pain-related behavior is similar to the result in this study.

In the clinical situation, nerve root infiltration (NRI) is used for nonsurgical treatment of radicular symptoms caused by LDH. Although a local anesthetic is effective for about 2 hours, some patients obtain relief from their symptoms for a few weeks or months after NRI. The mechanism is not completely understood, but a decrease in intraradicular blood flow [59, 60] and reduction in nerve conduction velocity [59] are associated with radiculopathy. A local anesthetic, or a combination of a local anesthetic and corticosteroids, are used for NRI, although adding corticosteroids is a controversial issue in nerve block treatments. In our previous *in vivo* studies, corticosteroids reduce the blood flow in the nerve root[61], and no additional benefit from using corticosteroids was identified[62]. In contrast, lidocaine has a longer-lasting effect in NRI, and therefore, an ion channel blocker is a potential agent for NRI. According to

the results in this study, administration of APETx2 involves the same procedure as NRI. Therefore, APETx2 or a combination of APETx2 plus a local anesthetic may be a potential agent for use in NRI for patients with LDH, especially in the early stage of the extruded type of LDH. However, APETx2 has not been tested in humans. We chose the APETx2 concentration according to a published paper[41]. A suitable concentration of APETx2 has not been established for clinical use. In addition, the timing of APETx2 administration should be investigated. Another limitation of our study is that the NP was a jelly-like viscous substance, and therefore, the ASIC3 level and NP cell apoptosis in the applied NP could not be examined during the observed time periods.

CONCLUSION

We demonstrated that APETx2 had an effect on pain-related behavior resulting from application of the NP to DRGs. In the clinical situation, this ASIC3 channel inhibitor could be a potential therapeutic agent for NRI in early-stage LDH.

REFECENCES

1. McCulloch JA. Focus issue on lumbar dis herniation: macro-and microdiscectomy. Spine 1996; 21:45S-56S.
2. Boden SD, Davis DO, Dina TS, et al. Abnormal magnetic-resonance scans of the lumbar spine in asymptomatic subjects. A prospective investigation. J Bone Joint Surg Am 1900; 72: 403-8.
3. Boos N, Rieder R, Schade V, et al. 1995 Volvo Award in clinical sciences. The diagnostic accuracy of magnetic resonance imaging, work perception, and psychosocial factors in identifying symptomatic disc herniation. Spine 1995; 20: 2613-25.
4. Aoki Y, Rydevik B, Kikuchi S et al. Local applications of disc-related cytokines on spinal nerve roots. Spine 2002;27:1614–1617
5. Igarashi T, Kikuchi S, Shuvayev V et al. Exogenous tumor necrosis factor-alpha mimics nucleus pulposus-induced neuropathology : molecular, histologic, and behavioral comparisons in rat. Spine 2000;25:2975–2980
6. Kayama S, Konno S, Olmarker K et al. Incision of the annulus fibrosus induces nerve root morphologic, vascular, and functional changes: an experimental study. Spine 1996;21:2539–2543
7. Kawakami M, Tamaki T, Weinstein JN et al. Pathomechanism of pain-related behavior produced by allografts of intervertebral disc in the rat. Spine 1996;21:2101–2107
8. Olmarker K, Rydevik B, Nordborg C. Autologous nucleus pulposus induces neurophysiologic and histologic changes in porcine cauda equine nerve roots. Spine 1993;18:1425–1432
9. Olmarker K, Brisby H, Yabuki S et al. The effects of normal, frozen, and hyaluronidase-digested nucleus pulposus on nerve root structure and function. Spine 1997;22:471–476
10. Olmarker K, Myers RR. Pathogenesis of sciatic pain: role of herniated nucleus pulposus and deformation of spinal nerve root and dorsal root ganglion. Pain 1998;78:99–105
11. Olmarker K, Larsson K. Tumor necrosis factor alpha and nucleus pulposus induced nerve root injury. Spine 1998;23:2538–2544

12. Onda A, Murata Y, Rydevik B et al. Immunoreactivity of brain-derived neurotrophic factor in rat dorsal root ganglion and spinal cord dorsal horn following exposure to herniated nucleus pulposus. Neurosci Lett 2003;352:49–52
13. Peng B, Wu W, Li Z et al. Chemical radiculitis. Pain 2007;127:11–16
14. Kato K, Kikuchi S, Konno S et al. Participation of 5-hydroxytryptamine in pain-related behavior induced by nucleus pulposus applied on the nerve root in rats. Spine 2008;33:1330–1336
15. Otoshi K, Konno S, Kato K et al. Anti-HMGB1 Neutralization Antibody Improves Pain-Related Behavior Induced by Application of Autologous Nucleus Pulposus Onto Nerve Roots in Rats. Spine 2011; 11: E692–E698
16. Weurtz K, Quero L, Sekiguchi M et al. The Red Wine Polyphenol Resveratrol Shows Promising Potential for the Treatment of Nucleus Pulposus–Mediated Pain *In Vitro and In Vivo.* Spine 2011; 21:E1373-84
17. Saito H, Wakai J, Sekiguchi M et al.The effect of selective serotonin reuptake inhibitor (SSRI) on pain-related behavior in a rat model of neuropathic pain. Eur Spine J 2014; 23:2401-2409
18. Handa J, Sekiguchi M, Olga Krupkova et al. The effect of serotonin–noradrenaline reuptake inhibitor duloxetine on the intervertebral disk-related radiculopathy in rats. Eur Spine J 2015; DOI 10.1007/s00586-015-4239-9
19. Kobayashi H, Kikuchi S, Konno S et al. Interaction of 5-Hydroxytryptamine and Tumor Necrosis Factor-α to Pain-Related Behavior by Nucleus Pulposus Applied on the Nerve Root in Rats. Spine 2011; 3: 210–218
20. Yabuki S, Kikuchi S, Olmaler K, et al. Acute effects of nucleus pulposus on blood flow and endoneurial fuid pressure in rat dorsal root ganalion. Spine 1998; 23: 2517-23.
21. Miyoshi S, Sekiguchi M, Konnno S et al. Increased Expression of Vascular Endothelial Growth Factor Protein in Dorsal Root Ganglion Exposed to Nucleus Pulposus on the Nerve Root in Rats. Spine 2010;36:E1-6
22. Reeh PW, Steen KH. Tissue acidosis in nociception and pain. Prog Brain

Res 1996;113: 143–151
23. Waxman SG, Dib-Hajj S, Cummins TR, et al. Sodium channels and pain. Oeic, Natl, Acad. Sci. USA 1999: 96: 7635-9.
24. Sulayman D, Dib-Hajj S, Joel Am et al. Voltage-gated sodium channels: Therapeutic targets for pain. Pain Med. 2009; 10: 1260-9.
25. de Weille JR, Bassilana F, Lazdunski M et al. Identification, functional expression and chromosomal localization of a sustained human proton-gated cation channel. FEBS Lett 1998;433:257-60
26. Waldmann R, Lazdunski M. H(+)-gated cation channels: neuronal acid sensors in the NaC/DEG family of ion channels. Curr Opin Neurobiol 1998;8: 418–424
27. Babinski K, Lê KT, Séguéla P et al. Molecular cloning and regional distribution of a human proton receptor subunit with biphasic functional properties. J Neurochem 1999;72:51-7
28. Benson CJ, Eckert SP, McCleskey EW. Acid-evoked currents in cardiac sensory neurons: a possible mediator of myocardial ischemic sensation. Circ Res 1999;84: 921–928
29. Kress M, Zeilhofer HU. Capsaicin, protons and heat: new excitement about nociceptors. Trends Pharmacol Sci 1999;20: 112–118
30. Pan HL, Longhurst JC, Eisenach JC et al. Role of protons in activation of cardiac sympathetic C-fibre afferents during ischaemia in cats. J Physiol 1999;518: 857–866
31. Sutherland SP, Benson CJ, Adelman JP et al. Acid-sensing ion channel 3 matches the acid-gated current in cardiac ischemia-sensing neurons. Proc Natl Acad Sci USA 2001;98: 711–716
32. Voilley N, de Weille J, Mamet J et al. Nonsteroid anti-inflammatory drugs inhibit both the activity and the inflammation-induced expression of acid-sensing ion channels in nociceptors. J Neurosci 2001;21: 8026–8033
33. Mamet J, Baron A, Lazdunski M, Voilley N. Proinflammatory mediators, stimulators of sensory neuron excitability via the expression of acid-sensing ion channels. J Neurosci 2002;22: 10662–10670
34. Ugawa S, Ueda T, Ishida Y, Nishigaki M et al. Amiloride-blockable acid-

sensing ion channels are leading acid sensors expressed in human nociceptors. J Clin Invest 2002;110: 1185–1190
35. Krishtal O. The ASICs: signaling molecules? Modulators? Trends Neurosci 2003;26: 477–483
36. Waldmann R, Bassilana F, De Weille JR et al. Molecular cloning of a non-inactivating proton-gated Na+ channel specific for sensory neurons. J Biol Chem 1997;272: 20975–20978
37. Voilley N, de Weille J, Mamet J et al. Nonsteroid anti-inflammatory drugs inhibit both the activity and the inflammation-induced expression of acid-sensing ion channels in nociceptors. J Neurosci 2001;21: 8026–8033
38. Ohtori S, Inoue G, Koshi T, et al. Up-regulation of acid-sensing ion channel 3 in dorsal root ganglion neurons following application of nucleus pulposus on nerve root in rats. Spine 2006;31:2048-52
39. Diochot S, Baron A, Rash LD, et al. A new sea anemone peptide, APETx2, inhibits ASIC3, a major acid-sensitive channel in sensory neurons. EMBO J 2004;23:1516-25
40. Xu S, Tu W, Wen Jet al. The selective ASIC3 inhibitor APETx2 alleviates gastric mucosal lesion in the rat. Pharmazie 2014;69:542-6
41. Izumi M, Ikeuchi M, Ji Q et al. Local ASIC3 modulates pain and disease progression in a rat model of osteoarthritis. J Biomed Sci 2012;19:77
42. Deval E, Noël J, Gasull X et al. Acid-sensing ion channels in postoperative pain. J Neurosci 2011;31:6059-66
43. Waldmann R, Champigny G, Bassilana F et al. A proton-gated cation channel involved in acid-sensing. Nature 1997; 386: 173–177
44. Chen CC, England S, Akopian AN et al. A sensory neuron-specific, proton-gated ion channel. Proc Natl Acad Sci USA 1998; 95: 10240–10245
45. Price MP, Snyder PM, Welsh MJ. Cloning and expression of a novel brain Na+ channel. J Biol Chem 1996; 271: 7879–7882
46. Waldmann R, Champigny G, Voilley N et al. The mammalian degenerin MDEG, an amiloride-sensitive cation channel activated by mutations causing neurodegeneration in Caenorhabditis elegans. J Biol Chem

1996; 271: 10433–10436
47. Lingueglia E, de Weille JR, Bassilana F et al. A modulatory subunit of acid sensing ion channels in brain and dorsal root ganglion cells. J Biol Chem 1997; 272: 29778–29783
48. Akopian AN, Chen CC, Ding Y et al. A new member of the acid-sensing ion channel family. Neuroreport 2000; 11: 2217–2222
49. Grunder S, Geissler HS, Bassler EL et al. A new member of acid-sensing ion channels from pituitary gland. Neuroreport 2000; 11: 1607–1611
50. Takebayashi T, Cavabaygh JM, Cuneyt OA, et al. Effect of nucleus pulposus on the neural actibity of dorsal root ganglion. Spine 2001; 26: 940-4.
51. Anzai H, Hamba M, Onda A, et al. Epidural application of nucleus pulposus enhances nociresponses of rat dorsal horn neurons. Spine 2002; 27: E50-D55.
52. Blanchard MG, Rash LD, Kellenberger S. Inhibition of voltage-gated Na(+) currents in sensory neurons by the sea anemone toxin APETx2. Br J Pharmacol 2012;165:2067-77
53. Watanabe K, Larsson K, Rydvik Bjorn et al. Increase of Sodium Channels (Nav 1.8 and Nav 1.9) in Rat Dorsal Root Ganglion Neurons Exposed to Autologous Nucleus Pulposus. The Open Orthopaedics Journal 2014; 8:69-73
54. Wuertz K, Quero L, Sekiguchi M, et al. The red wine polyphenol resveratrol show promising potential for the treatment of nucleus pulposus-mediated pain *in vitro* and *in vivo*. Spine 2011; 36: E1373-84.
55. Krupkova O, Sekiguchi M, Klasen J, et al. Epigallocatechin 3-gallate suppresses interleukin-1-induced inflammatory responses in intervertebral disc cells in vitro and reduces radiculopathic pain in rats. Eur Cell Mater 2014; 28:372-86.
56. Kato K, Kikuchi S, Konno S et al. Participation of 5-Hydroxytryptamine in Pain-Related Behavior Induced by Nucleus Pulposus Applied on the Nerve Root in Rats. Spine 2011; 12: 1330–1336
57. Uchiyama Y, Cheng CC, Danielson KG, et al. Expression of acid-sensing ion channel 3 (ASIC3) in nucleus pulposus cells of the intervertebral disc

is regulated by p75NTR and REK signaling. J Bone Miner Res 2007; 22: 1996-2006.
58. Sun X, Jin J, Zhang JG, et al. Expression of acid-sensing ion channels in nucleus pulposus cells of the human intervertebral disk is regulated by non-steroid anti-inflammatory drugs. Acta Biochim Biophys Sin 2014; 46: 774-81.
59. Yabuki S, Kawaguchi Y, Nordborf C, et al. Effect of lidocaine on nucleus polposus-induces nerve root injury: A neurophysiologic and histologic study of the pig cauda equine. Spine 1998; 23: 1383-9.
60. Onda A, Yabuki S, Kikuchi S, et al. Effect of lidocaine on blood flow and endoneurical fluid pressure in a rat model of herniated nucleus pulposus. Spine 2001; 26: 2186-92.

Table 1

Table 1 The number of rats in each experimental group at each time point

Experimental groups n (total)=183			**Analysis**	**Day0**	**Day2**	**Day7**	**Day14**	**Day21**	**Day28**
Naive n=3			IB:n=3						
Non-treatment Group	NP n=6		IHC:n=6	*np*	*np*	*np*	n=6	*np*	*np*
	Sham n=6		IHC:n=6	*np*	*np*	*np*	n=6	*np*	*np*
Treatment group	NP n=168	SM n=42	vF:n=12	n=12	n=12	n=12	n=12	n=12	n=12
			IHC:n=6	*np*	*np*	*np*	n=6	*np*	*np*
			IB:n=24	*np*	*np*	n=6	n=6	n=6	n=6
		LD n=42	vF:n=12	n=12	n=12	n=12	n=12	n=12	n=12
			IHC:n=6	*np*	*np*	*np*	n=6	*np*	*np*
			IB:n=24	*np*	*np*	n=6	n=6	n=6	n=6
		MD n=42	vF:n=12	n=12	n=12	n=12	n=12	n=12	n=12
			IHC:n=6	*np*	*np*	*np*	n=6	*np*	*np*
			IB:n=24	*np*	*np*	n=6	n=6	n=6	n=6
		HD n=42	vF:n=12	n=12	n=12	n=12	n=12	n=12	n=12
			IHC:n=6	*np*	*np*	*np*	n=6	*np*	*np*
			IB:n=24	*np*	*np*	n=6	n=6	n=6	n=6

SM: solving medium, *LD*: low-dose APETx2, *MD*: middle-dose APETx2, *HD*: high-dose APETx2, *vF*: von Frey test, *IHC*: immunohistochemistry, *IB*: immunoblotting

Figure leadings

Fig.1Behavioral testing among 4 groups [SM ; solvating media, LD ; low dose (0.01μg), MD ; middle dose (0.1μg), HD ; high dose (1.0μg)].

In the SM group, the mechanical withdrawal threshold decreased at Day 7 and remained low until Day 28. In the HD group, the threshold significantly improved at Days 14 and 21 compared to the SM group ($p<0.05$). In the MD group, the threshold was significantly increased at Day 14 ($p<0.05$), but not at Day 28 compared to the SM group. We found no significant differences in the withdrawal threshold between the SM and LD groups.

Fig. 2

Expression of ASIC3 in the left L5 DRG.

We found no significant differences in ASIC3 intensity among the treatment groups at any time point.

Fig.3

The ratio of NGF-IR neurons in DRG.

a. NGF-IR DRG neurons were expressed in the NP and Sham groups (Day7) (Scale bar 50μm). On Days 7 and 14, the ratio of NGF-IR neurons in the NP group was significantly higher in the Sham group ($p<0.05$).
b. NGF-IR DRG neurons were expressed in four treatment groups (Day7) (Scale bar 50μm). The ratio of NGF-IR neurons in DRG of the treatment groups. In the MD and HD groups, the ratio of NGF-IR neurons in DRG was significanlty lower than other two groups ($p<0.05$).

Fig.4

The ratio of ATF3-IR neurons in DRG.

a. ATF3-IR DRG neurons were expressed in the NP group and a few ATF3-IR was observed in the Sham group (Day7) (Scale bar 50μm). On Days 7and 14, the ratio of ATF3-IR neurons in the NP group was significantly higher in the Sham group ($p<0.05$).
b. ATF3-IR neurons and satellite cells were observed in all treatment groups (Day

7) (Scale bar 50μm). The ratio of ATF3-IR neurons in DRG of the treatment groups. There were no significant difference of the ratio of ATF3-IR neurons in DRG at any time point.

Fig. 5　The ratio of HIF-1α-IR neurons in DRG.

a.　HIF-1α-IR in DRG (Day 14). HIF-1α-IR in the NP (non-treatment) group was observed in the DRG at days 14. Some cytoplasm of DRG neuron cells were positive for HIF-1α (Scale bar: 50 μm).

b.　The ratio of HIF-1α-IR neurons. The ratio of HIF-1α-IR neurons was higher in the NP (non-treatment) group compared to that of Sham group ($p<0.05$)

Fig.6　The number of IBa1-IR neurons in SC.

a. Iba1-IR microglia was observed in the dorsal horn of the NP and Sham groups (Scale bar 200μm). The number of Iba1-IR microglia in the NP group was significantly higher in the Sham group at each time point ($p<0.05$).
b. Iba1-IR microglia was expressed in the dorsal horn of the NP and Sham groups. Morphological changes of activated microglia were observed (Scale bar 200μm). The number of Iba1-IR microglia in SC of the treatment groups. There was no significant difference of the number of Iba1-IR in SC at each time point.

Figure 1

Fig. 1

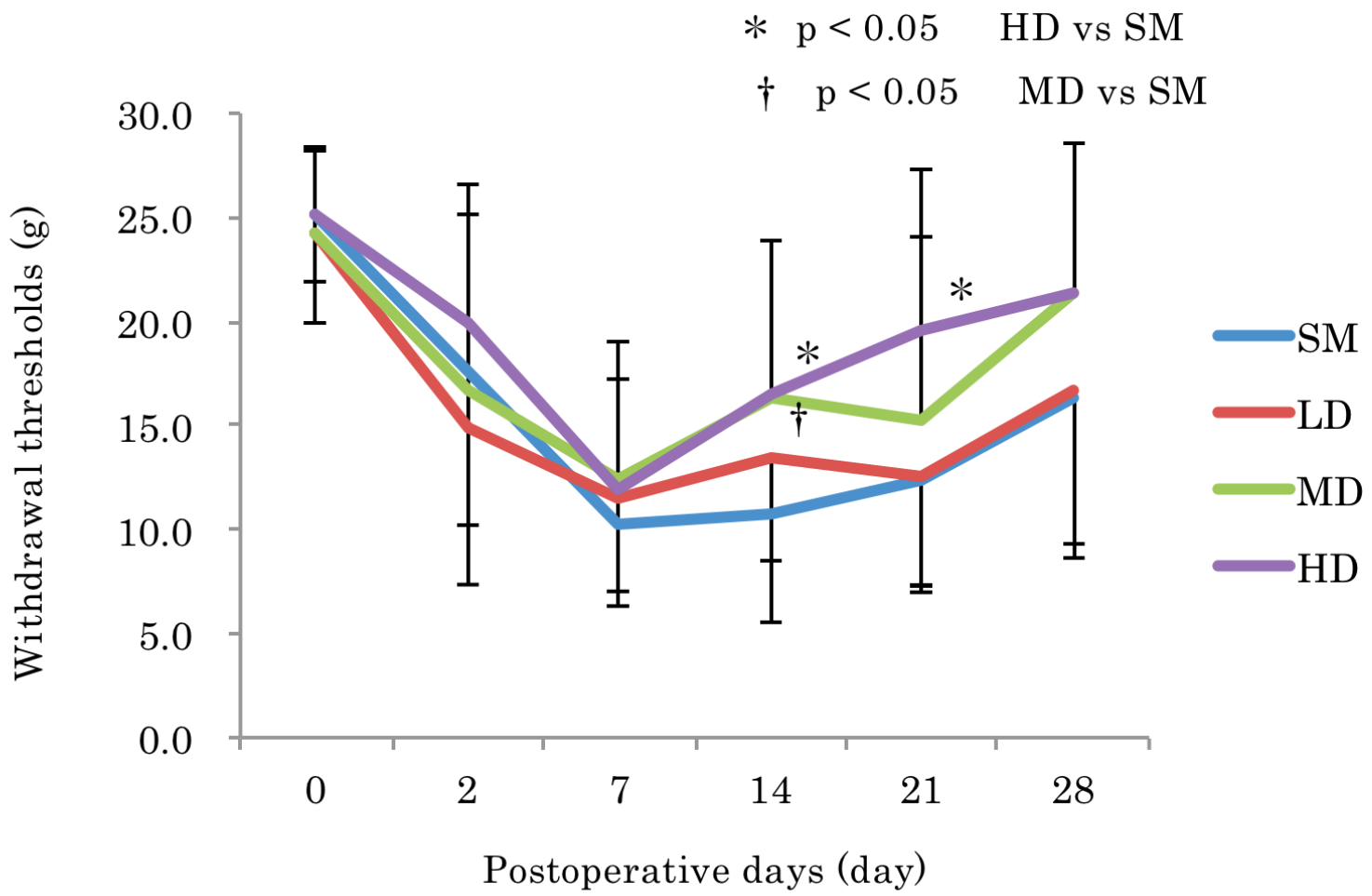

Figure 2

Fig. 2

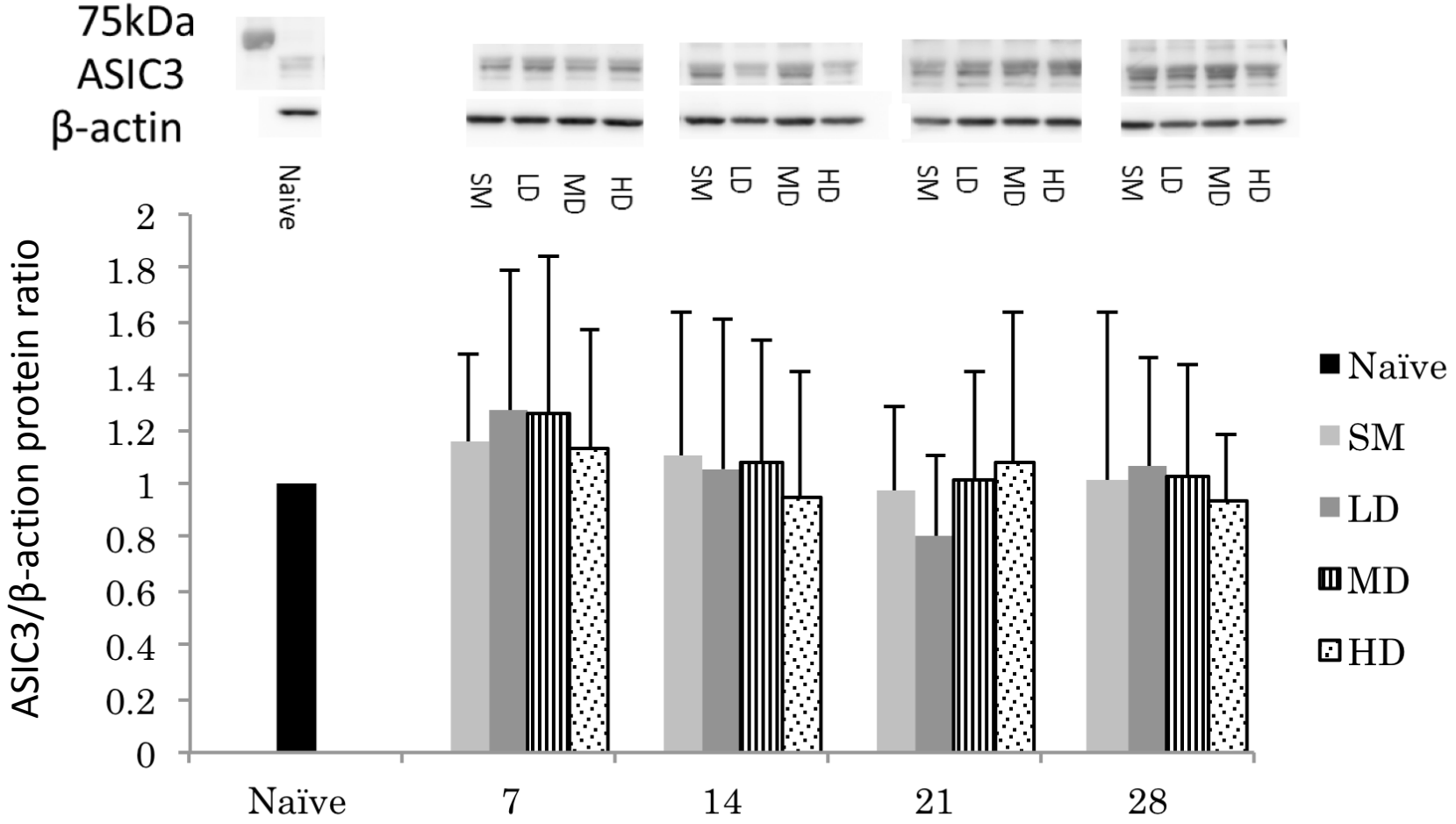

Figure 3a

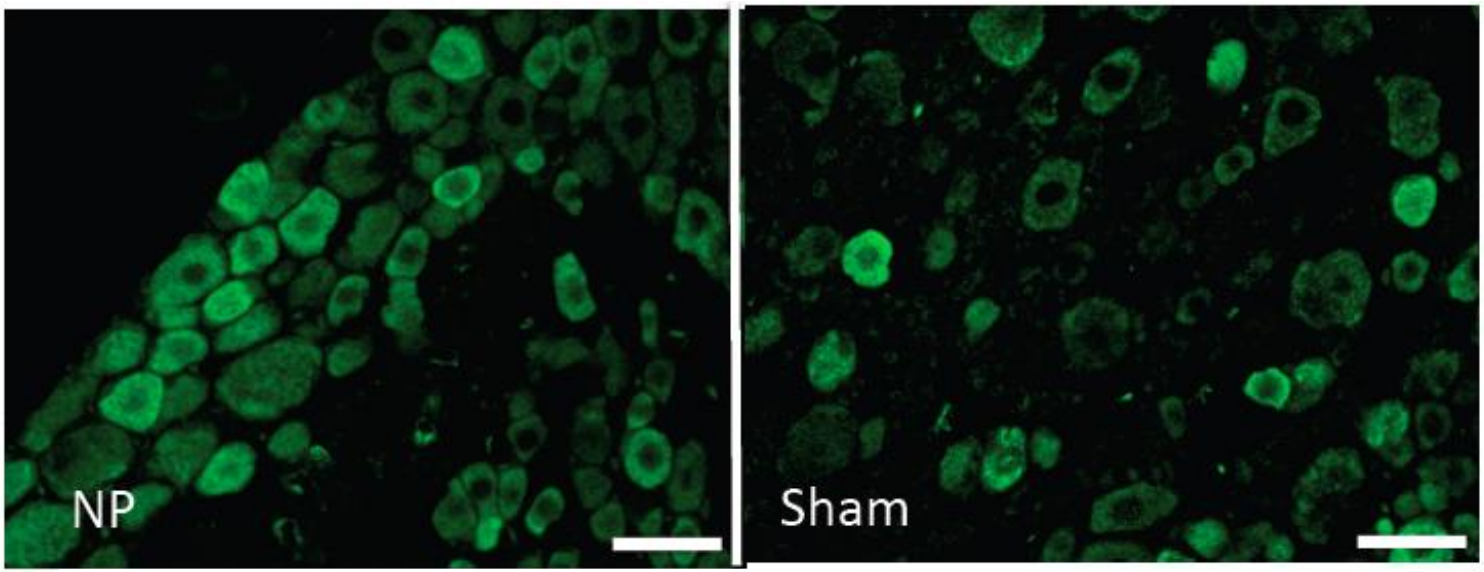
NP
Sham

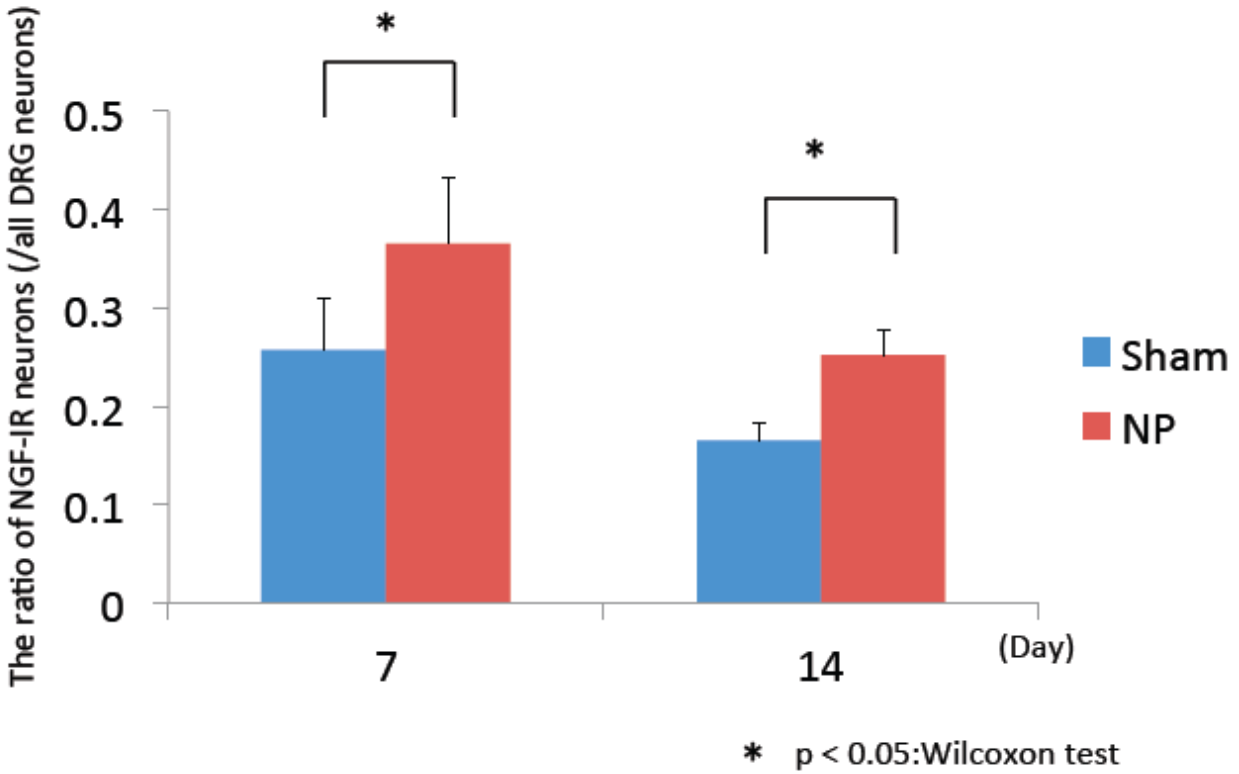
The ratio of NGF-IR neurons (/all DRG neurons)
0.5
0.4
0.3
0.2
0.1
0
*
*
7
14
(Day)
Sham
NP
* p < 0.05:Wilcoxon test

Figure 3b

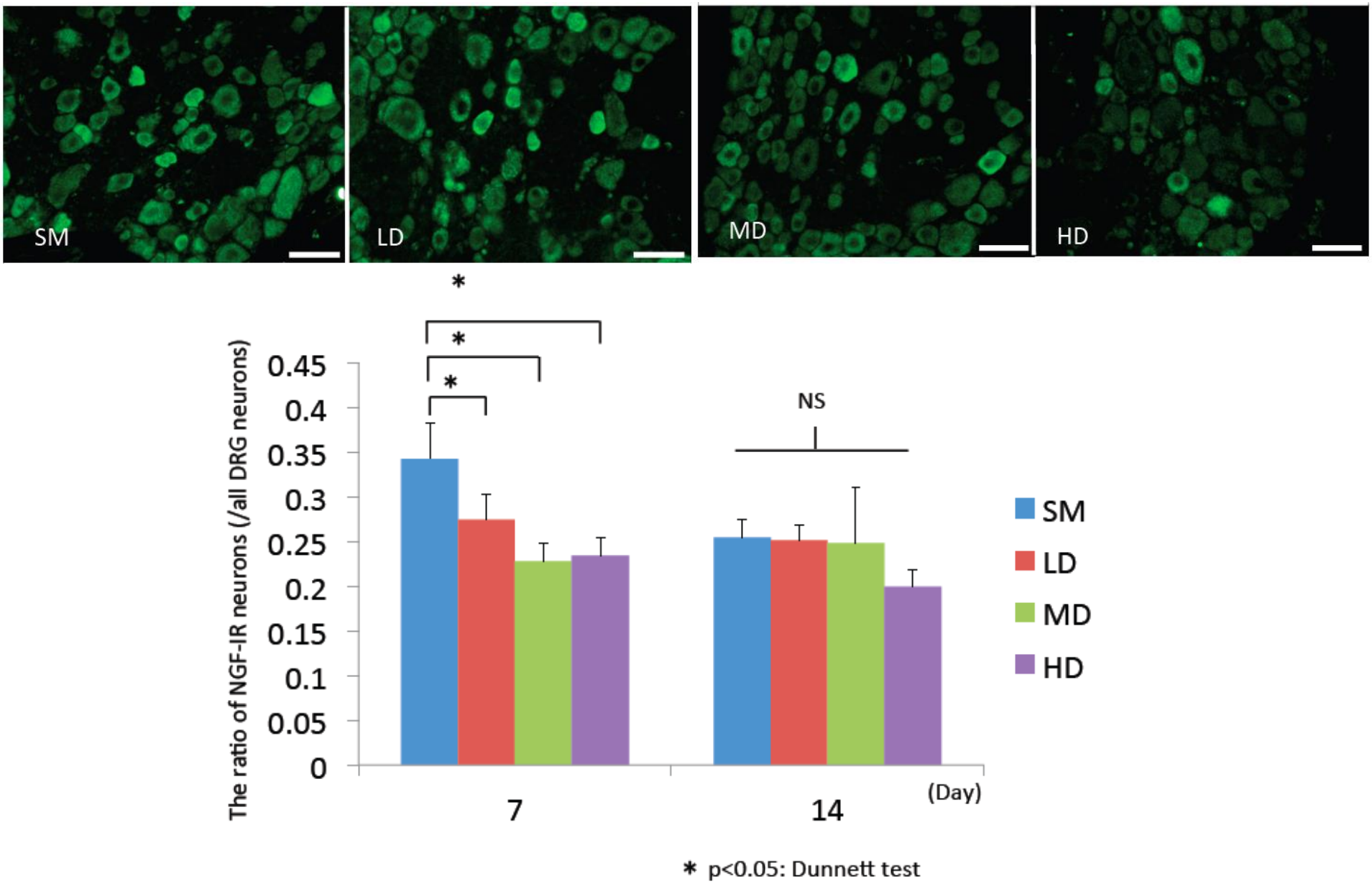
SM
LD
MD
HD
*
*
*
NS
The ratio of NGF-IR neurons (/all DRG neurons)
0.45
0.4
0.35
0.3
0.25
0.2
0.15
0.1
0.05
0
7
14
(Day)
SM
LD
MD
HD
* p<0.05: Dunnett test

Figure 4a

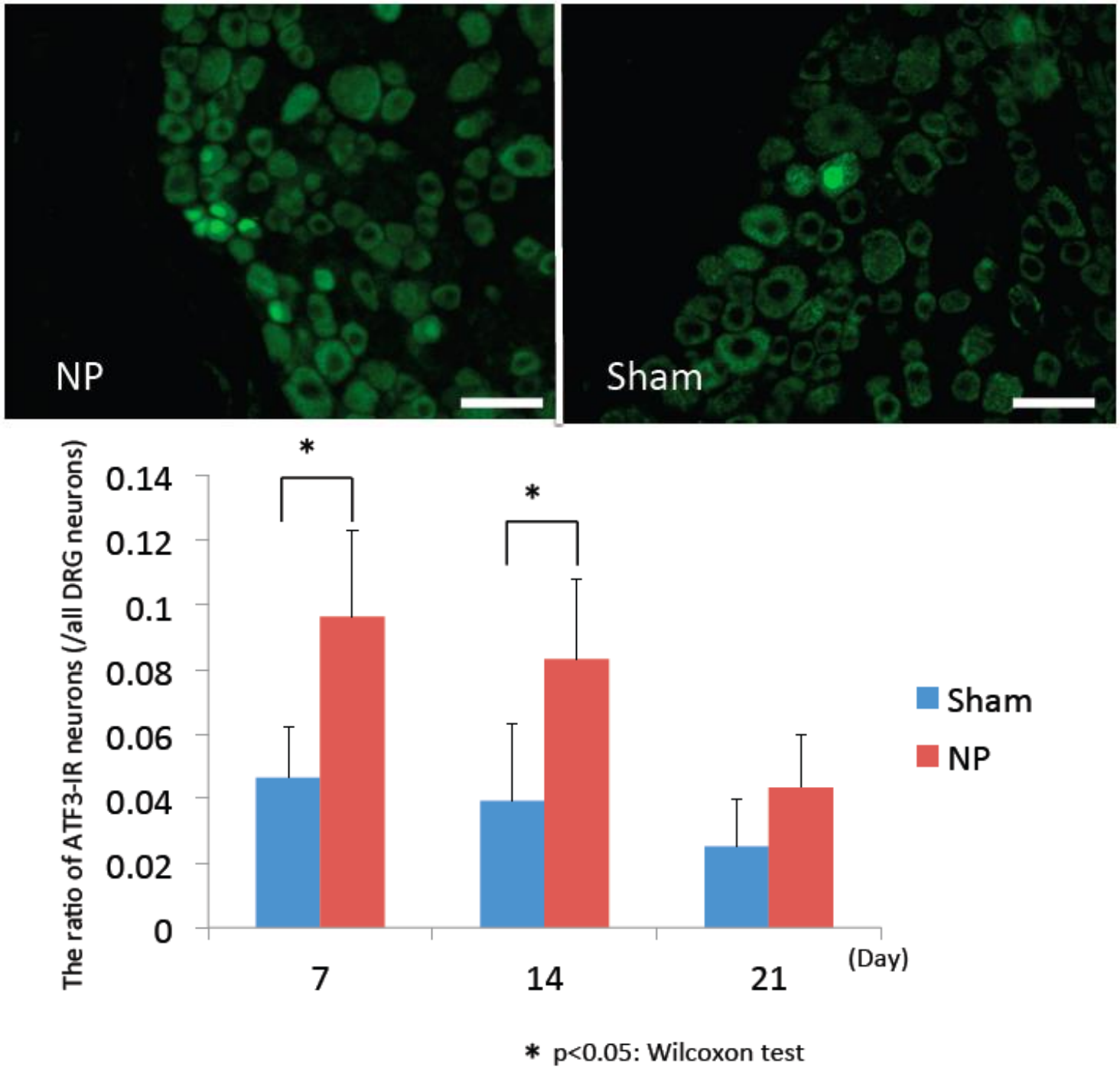
NP
Sham
The ratio of ATF3-IR neurons (/all DRG neurons)
0.14
0.12
0.1
0.08
0.06
0.04
0.02
0
*
*
7
14
21
(Day)
Sham
NP
* p<0.05: Wilcoxon test

Figure 4b

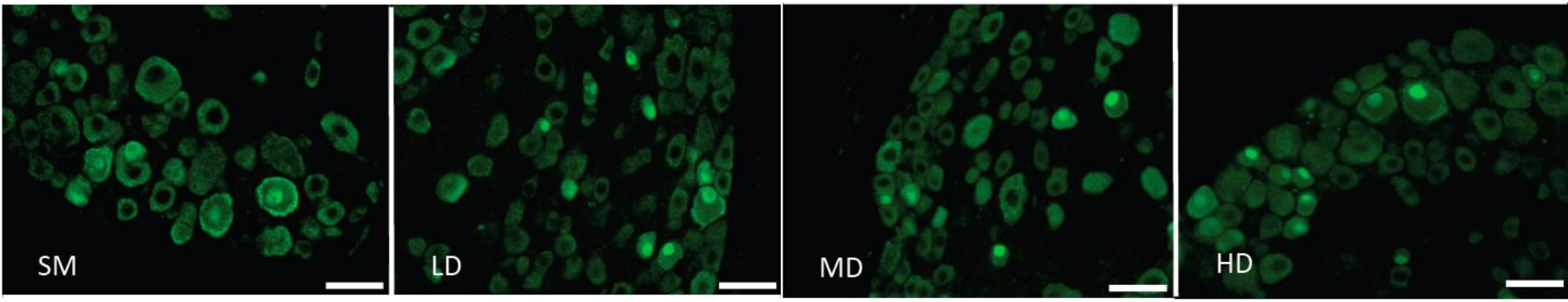
SM
LD
MD
HD

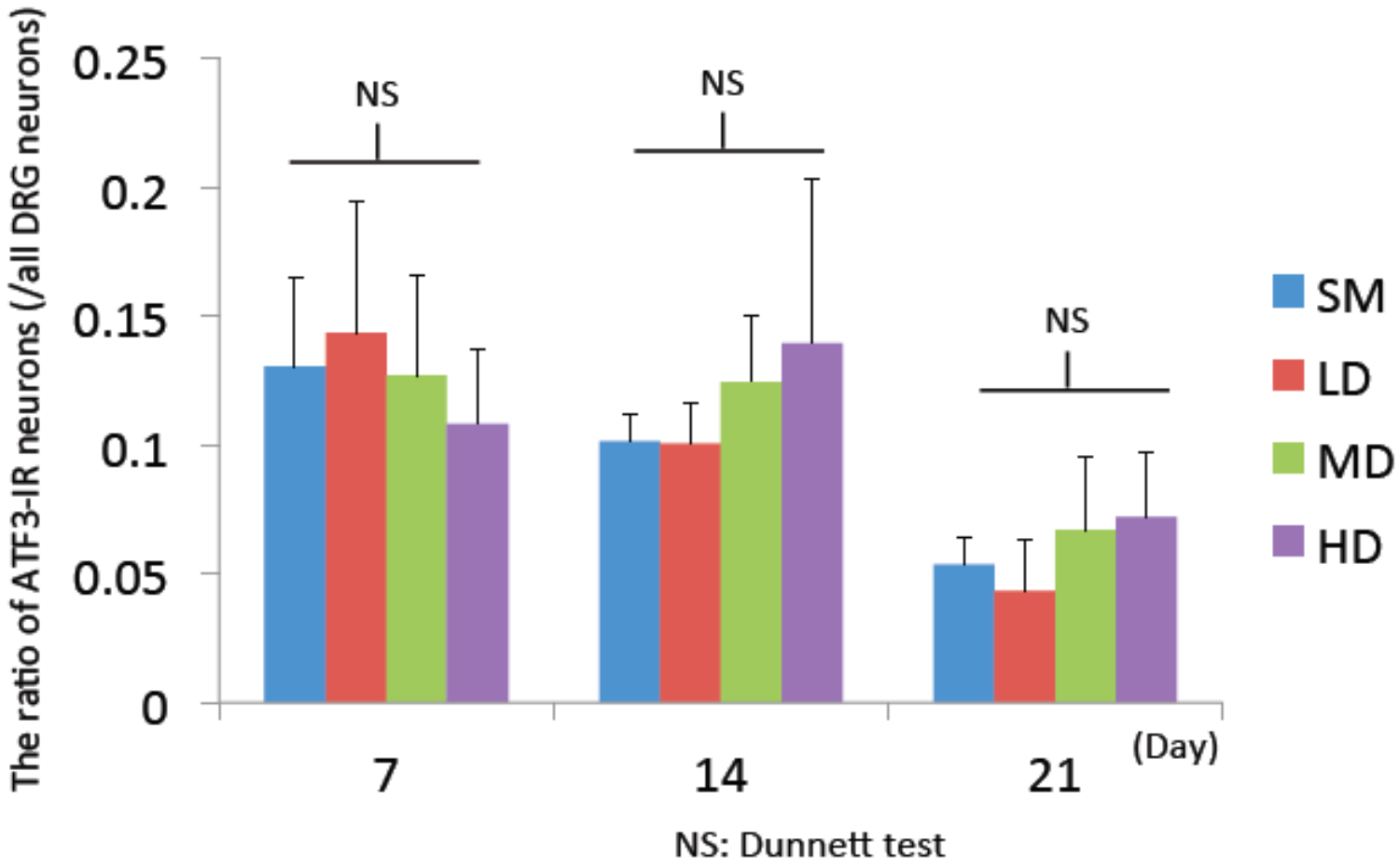
The ratio of ATF3-IR neurons (/all DRG neurons)
0.25
0.2
0.15
0.1
0.05
0
NS
NS
NS
7
14
21
(Day)
SM
LD
MD
HD
NS: Dunnett test

Figure 5a

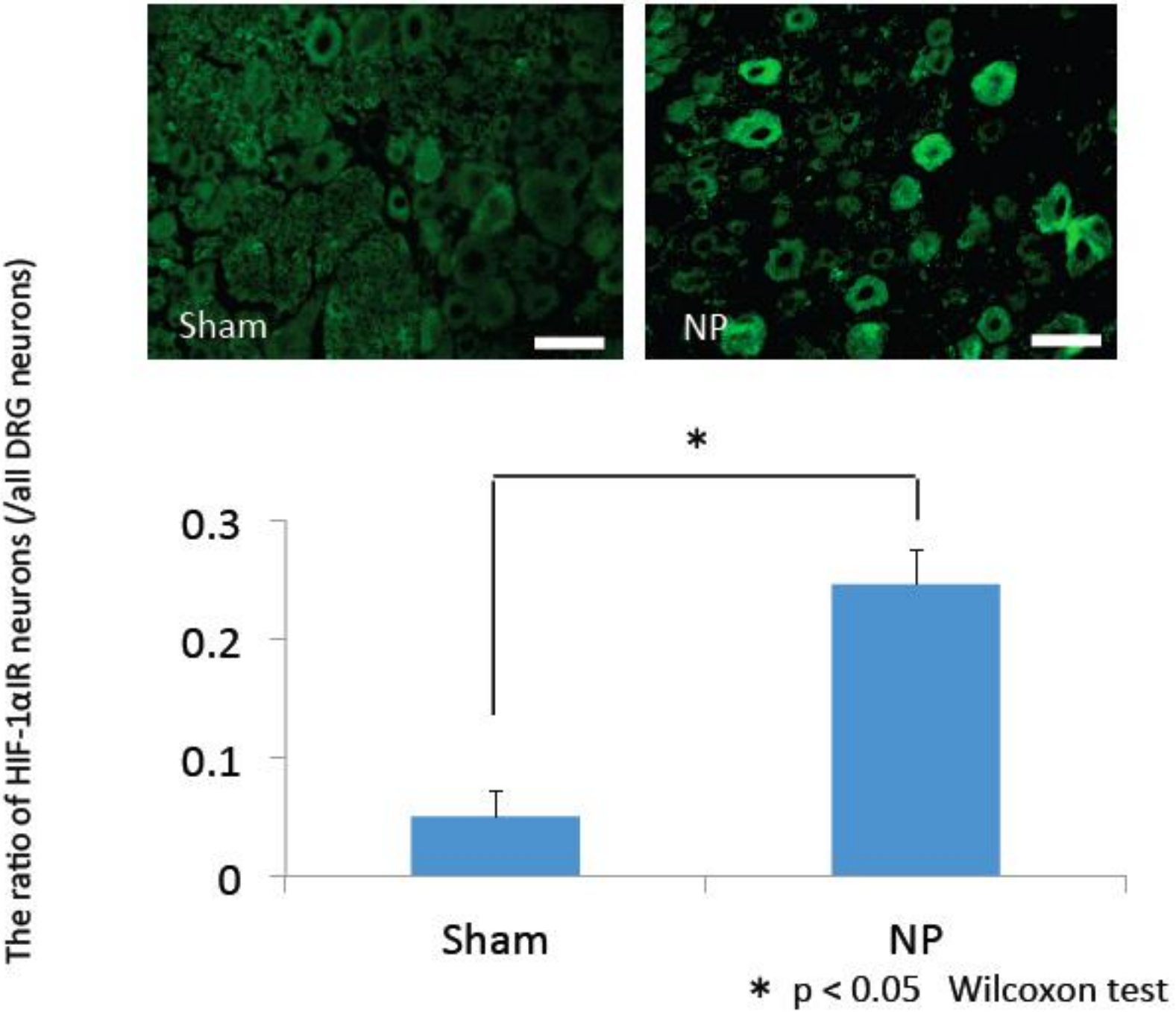
Sham
NP
*
0.3
0.2
0.1
0
The ratio of HIF-1αIR neurons (/all DRG neurons)
Sham
NP
* p < 0.05 Wilcoxon test

Figure 5b

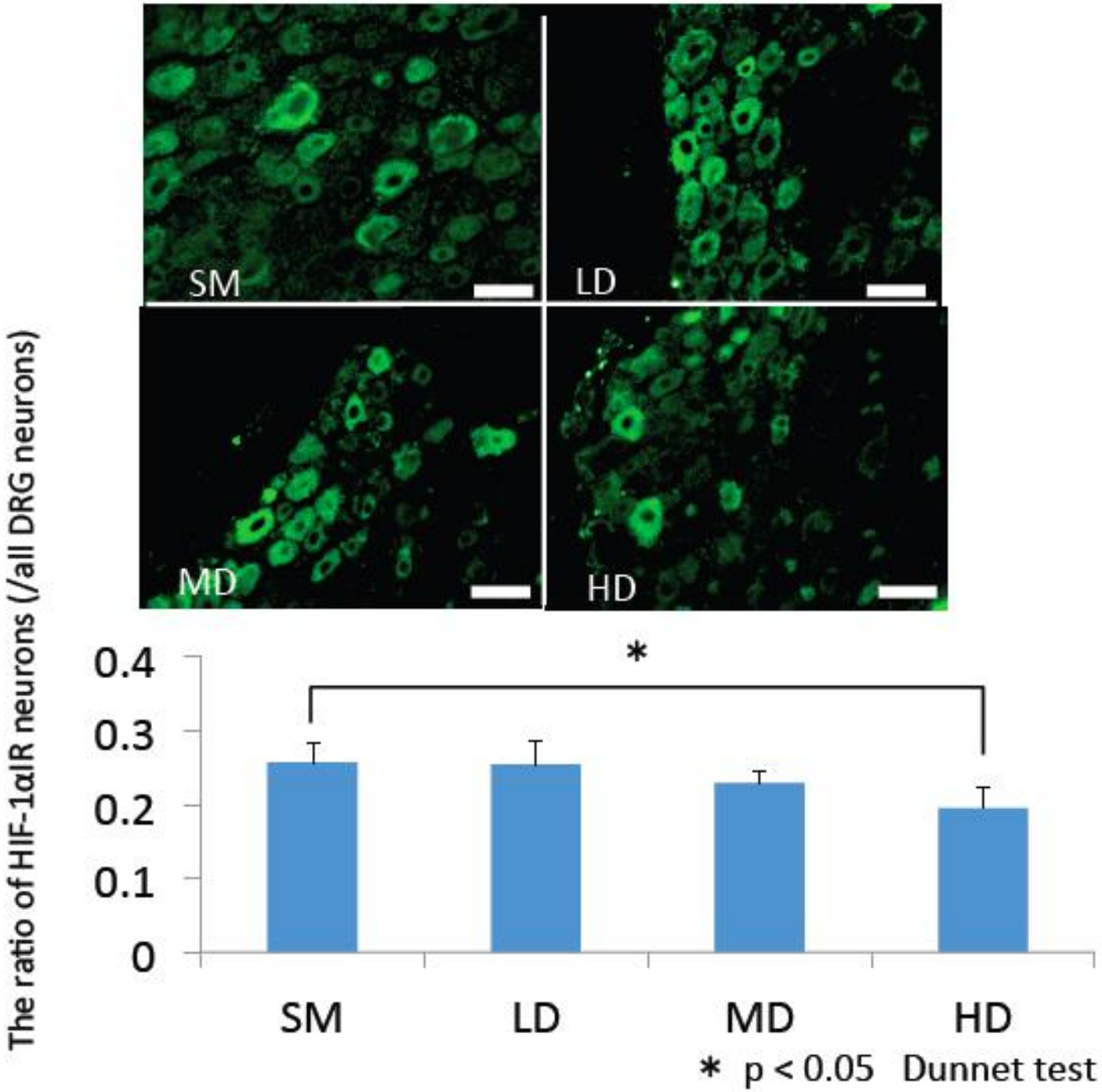
SM
LD
MD
HD
The ratio of HIF-1αIR neurons (/all DRG neurons)
0.4
0.3
0.2
0.1
0
*
SM
LD
MD
HD
* p < 0.05 Dunnet test

Figure 6a

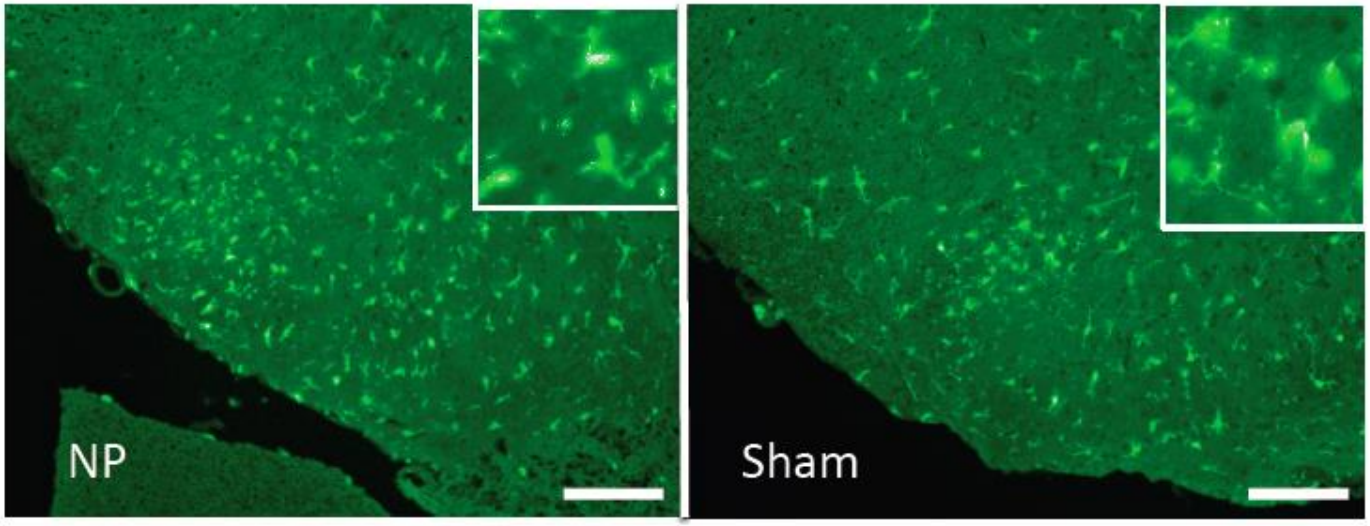
NP
Sham

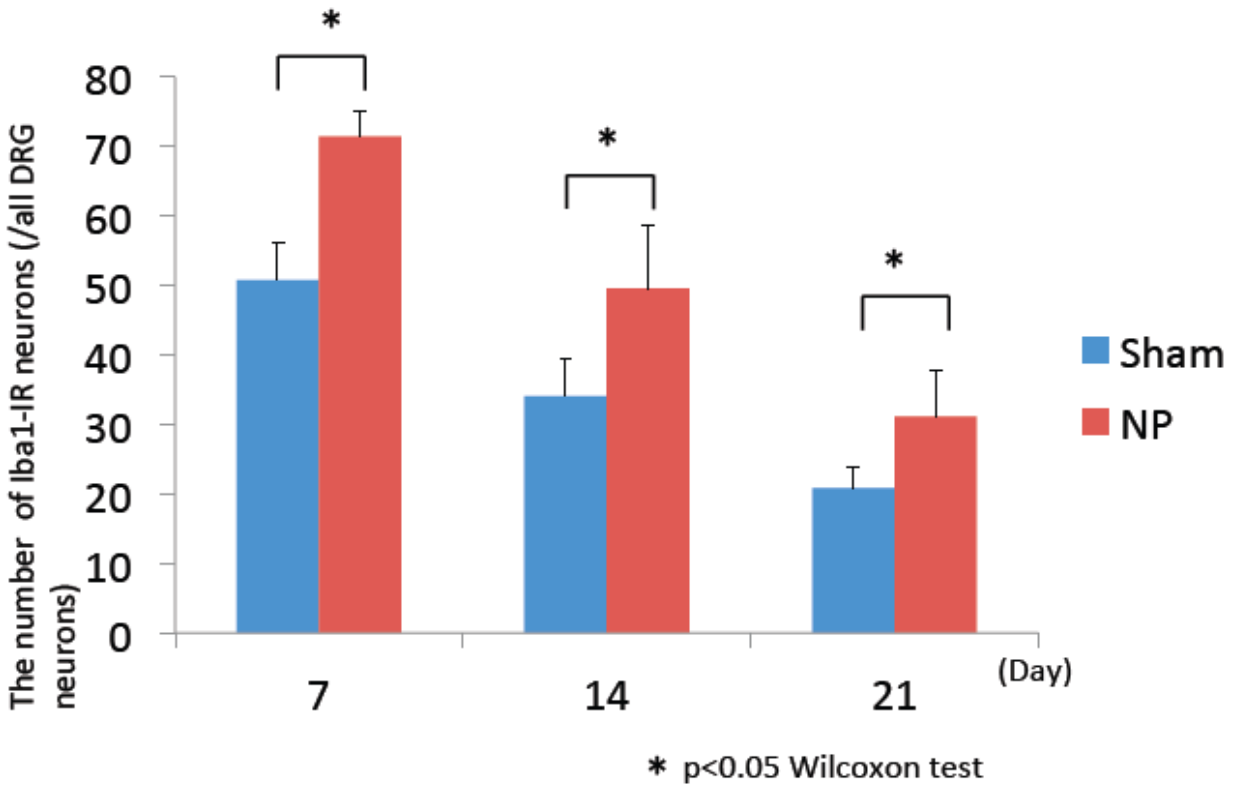
*
*
*
80
70
60
50
40
30
20
10
0
The number of Iba1-IR neurons (/all DRG neurons)
7
14
21
(Day)
Sham
NP
* p<0.05 Wilcoxon test

Figure 6b

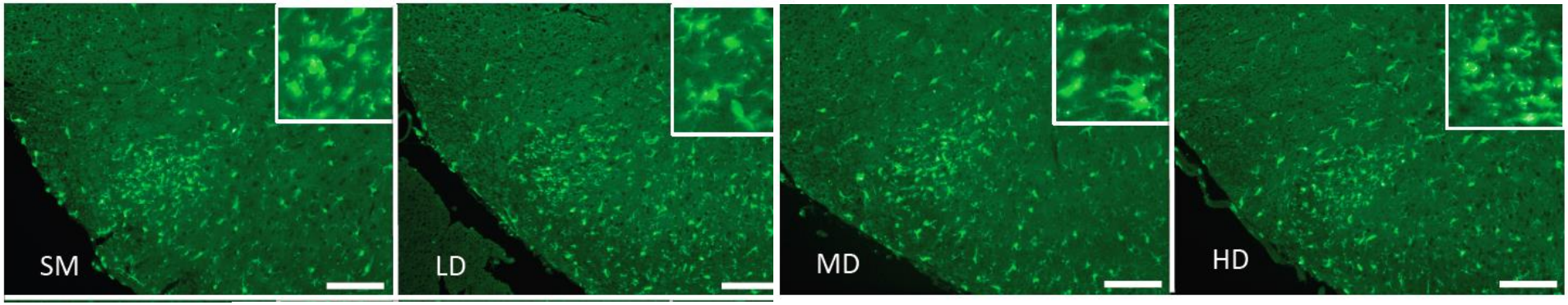
SM
LD
MD
HD

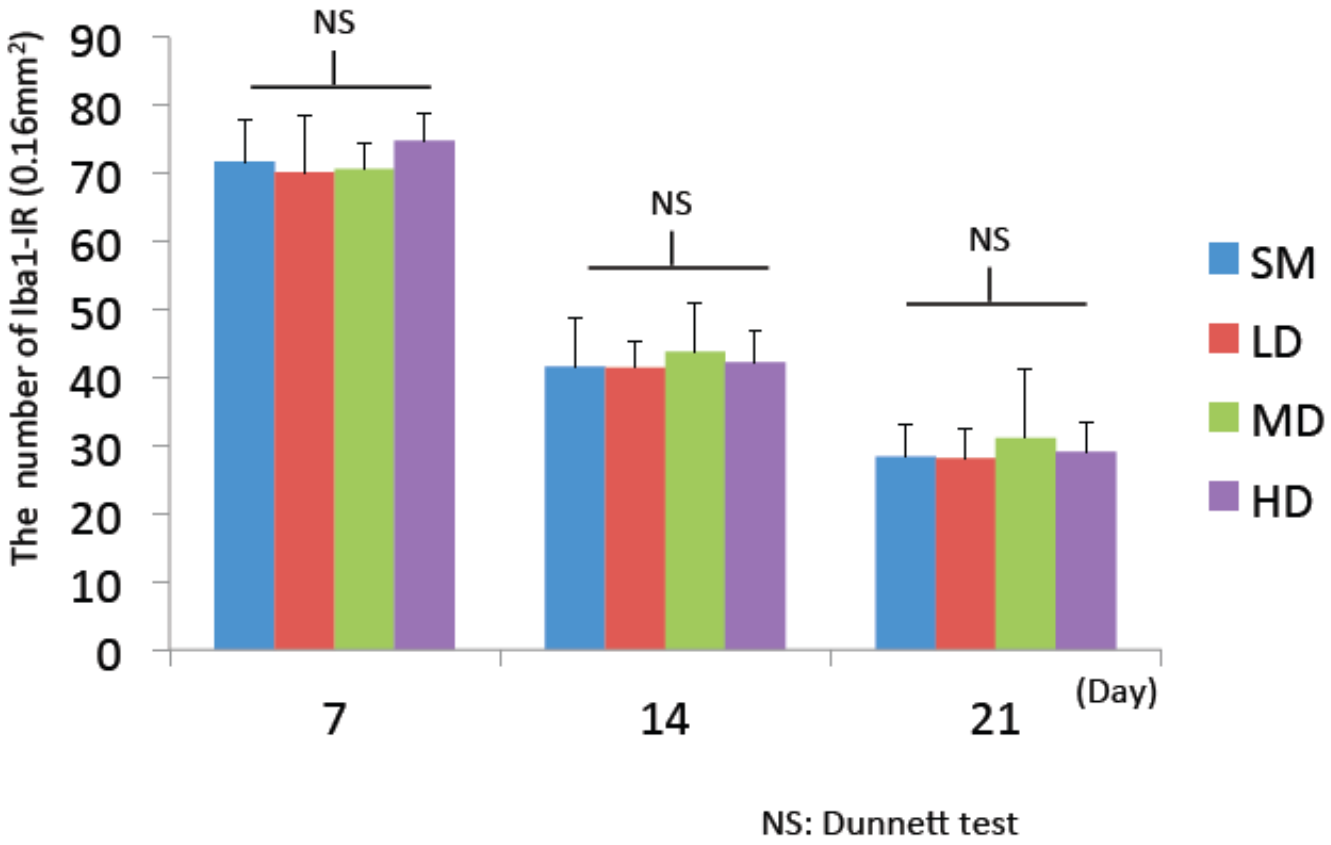
The number of Iba1-IR (0.16mm²)
90
80
70
60
50
40
30
20
10
0
NS
NS
NS
7
14
21
(Day)
SM
LD
MD
HD
NS: Dunnett test